Crystal-field magnetic anisotropy of dilute dysprosium or erbium in yttrium single crystals

J. Høg and P. Touborg
Department of Electrophysics, The Technical University of Denmark, DK-2800 Lyngby, Denmark
(Received 5 October 1973)

Magnetization measurements have been performed between 1.3 and 300 K in fields up to 50×10^5 A/m in the a, b, and c directions of hcp crystals of pure Y and Y doped with 0.14-at.% Dy or 0.14-at.% Er, using the Faraday method and a vibrating-sample method. The characteristic behavior of both the isothermal and isofield susceptibility curves could be interpreted in terms of a general single-ion anisotropy Hamiltonian and a molecular-field exchange model. In this way the following anisotropy parameters $A_{nm} \langle r^n \rangle$, with $(n, m) = (2, 0)$, $(4, 0)$, $(6, 0)$, and $(6, 6)$ respectively, were obtained (in units of K): Er, -122 ± 12, $+18.3 \pm 1.8$, $+11.7 \pm 1.2$, -135 ± 13; Dy, -50.5 ± 5, $+49.5 \pm 5$, $+40.4 \pm 4$, -321 ± 32. The higher-order anisotropy parameters play an important part in determining the crystal-field-level scheme and they are incompatible with a model assuming that the charges giving rise to the crystal field are solely external to the magnetic ion. The exchange interactions differ by up to a factor of 15 for c and basal-plane directions.

INTRODUCTION

The crystal-field anisotropy in the rare-earth metals and alloys plays a crucial part in determining their magnetic properties. A direct determination of the crystalline-field parameters in these materials is difficult because of contributions from anisotropic exchange and magnetostriction to the magnetic anisotropy, and also because the crystal-field splitting is generally smaller than the exchange energies, making exact theories of the exchange necessary.

To avoid these problems a program for determining crystal-field anisotropy of both light and heavy rare earths diluted in the nonmagnetic metals Y or Lu has been initiated. Y and Lu have been chosen because of the similarities of these metals to the magnetic rare-earth metals, including the crystal structure (hcp), the matching of lattice constants as illustrated in Table I for Dy and Er, and the electronic structure.

Only few data on magnetic measurements on rare earths diluted in Y or Lu are available. Sugawara and Soga[2] have briefly reported susceptibility measurements on polycrystalline samples of 0.5-at.% Er, Nd, and Tb in Y. Their measurements indicate a splitting between the ground state and the first excited state of about 15 K for Er.

In the present paper we report static magnetization measurements on single crystals of dilute alloys of Dy or Er in Y and fits of theoretical curves to these measurements. Both Dy and Er are expected to be tripositive ions with a ground-state multiplet with $J = \frac{15}{2}$. In a hexagonal crystal potential this multiplet will split into eight Kramers doublets, and with the low doping actually used, a nearly-single-ion paramagnetic behavior may be expected.

EXPERIMENTAL PROCEDURE

Magnetization measurements in the temperature range 1.3–300 K and the field range $0-50 \times 10^5$ A/m were performed on single-crystal spheres of pure Y, Y–0.14-at.% Dy, and Y–0.14-at.% Er, respectively. The single crystals were grown using sublimed 99.99%-purity Y and 99.9%-purity Dy and Er by the technique of annealing arc-melted buttons.[3,4] Spheres of 102.69 mg (Y-Dy), 250.5 mg (Y-Er), and 245.7 mg (Y) were made by spark cutting and oriented by x-ray Laue techniques. Table II lists the impurities in the Y metal, determined from a metallographic analysis. The magnetic contribution from the Y to the magnetic moment of the alloy samples was subtracted, giving the rare-earth impurity moment separately. Care was taken that the pure-Y sample measured was representative.

To get thorough and accurate measurements in the temperature and field ranges mentioned, it was necessary to use two different techniques for measuring magnetic moments. Both magnetometers made use of the same cryostat with a superconducting 52×10^5 A/m (65 kOe) magnet with vertical field. The accuracy of the magnetic field, which at low fields was measured using a magnetoresistance probe and at high fields deduced from the current flowing in the magnet, was $\pm 0.5\%$.

TABLE I. Lattice constants (Ref. 1) in units of Å.

	a	c	c/a
Y	3.650	5.741	1.5750
Dy	3.593	5.654	1.5735
Er	3.561	5.593	1.5706
Lu	3.510	5.567	1.5797

TABLE II. Impurities in the Y metal.

Impurity	ppm
Al	4
Ca	2
Cr	3
Cu	2
Fe	7
Mg	<1
Pb	20
Ag	1
Rare earths	not detected

The Faraday magnetometer, which was by far the most sensitive, utilizes a null-reading electronic balance and superconducting gradient coils. The maximum gradient field was 2.5×10^4 (A/m)/cm and the minimum weight which could be measured was 0.01 μg, giving rise to a sensitivity which was more than adequate for any magnetic moments which we measured. To make the measurements insensitive to gradients in the main field and to drift in the balance, the force was measured with the gradient field in the two opposite directions. The instrument was calibrated with a Ni sphere using the saturation values from Crangle and Goodman[5] and the accuracy on the magnetic-moment measurement was ±0.5% at low fields and ±1% at high fields. The contribution from the empty sampleholder was measured and subtracted. The temperature was varied by heating the sample tube (maximum 100 K) or by pumping on liquid He in a Dewar around the sample tube (minimum 1.3 K). Above 4.2 K the temperature was measured with an accuracy of ±0.1 K by a Ge resistor situated immediately below the sample and below 4.2 K by the pressure corresponding to the boiling point, accuracy ±0.05 K.

The Faraday magnetometer was used for measuring initial susceptibilities up to 100 K in all samples and isotherms in pure Y in both basal-plane and c-axis directions, and for measuring isotherms in the doped samples in the easy directions. Application of higher magnetic fields to the doped samples in the hard directions caused the sample to swing out to the walls of the sample chamber, disturbing the force measurement.

For these cases and for isofield magnetization measurements up to 300 K at 44.2×10^5 A/m for all samples a vibrating-sample magnetometer (VSM) was used. In this apparatus the sample was vibrating vertically with a frequency of 5 Hz between two vertical pickup coils. The induced signal in these was measured by a compensation technique. The sensitivity corresponded to a magnetic moment of $0.5\times10^{15}\mu_B$ and the accuracy was ±1%.

A Ni sphere was used for calibration. Two different sample holders were used: a low-temperature sample holder made of Tufnol, in which case the temperature was varied and measured in a similar way as in the Faraday magnetometer, and a high-temperature sample holder made of pure Cu and containing a heating coil and a thermocouple for measurements up to 300 K. The temperature accuracy in the high-temperature sample holder was ±0.5 K. The reason for using two sample holders was the relatively high contribution of the high-temperature version to the total susceptibility if used at low temperatures. The empty-sample-holder signals were subtracted but were difficult to reproduce and contributed about $\pm2.5\times10^{16}\mu_B$ to the uncertainty.

EXPERIMENTAL RESULTS

Curves of magnetization vs temperature and field are shown in Figs. 1–10 together with the theoretically fitted curves. The fits will be discussed later. In this section the experimental data with general features and comments only are presented. In Figs. 2–10 the unit for magnetic moment is Bohr magnetons per rare-earth (RE) atom.

Pure Y

The initial susceptibilities in the b axis and c axis (Fig. 1) follow a linear behavior at high temperatures but deviate from it at low temperatures, owing to impurities. The extrapolated high-temperature polycrystalline susceptibility per Y atom at 0 K is $3.98\times10^{-10}\mu_B/(\mathrm{A/m})$, in agreement with the value $3.88\times10^{-10}\mu_B/(\mathrm{A/m})$ obtained by Wohlleben.[6] The isothermal magnetization curves deviate slightly from linearity at low temperatures. The subtraction of the Y contribution in the alloy-sample measurements is essential and the uncertainty in the Y measurements gives, in some cases, rise to relatively large uncertainties in the rare-earth moment. The worst cases are the measurements in the hard directions at high temperatures and in the c direction in Y-Dy at low temperatures, where the Y contributes up to 75% of the total moment of the doped sample. In the former case the Y uncertainty (±1%) gives rise to an uncertainty ±3% in the rare-earth moment. At low temperatures the Y background is estimated to be determined to within ±2%, thus giving rise in the worst case (Y-Dy at 13 K) to an uncertainty ±6%.

0.14-at.% Dy and 0.14-at.% Er

The initial susceptibility in the basal-plane and c directions (Figs. 2 and 3) measured at a constant low field (1.35×10^5 A/m) show marked deviations from a Curie–Weiss behavior, this being most pronounced in the c-direction curve of Y-Dy (Fig. 3). The reproducibility of these measurements was checked by measuring the Y-Er sample twice with several months interval (Fig. 2, first and

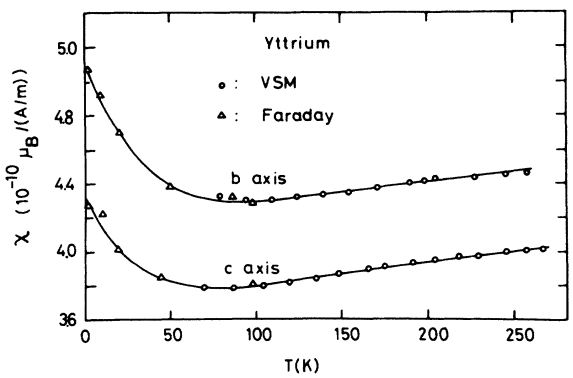

FIG. 1. Susceptibilities for pure Y in the b and c directions.

second run).

The isothermal magnetization curves in the easy directions, which are the c axis in Y-Er and the basal plane in Y-Dy (Figs. 4 and 5), show saturation at low temperatures at the fields available. The isotherms at low temperatures in Y-Dy (Fig. 5) were measured in both the a and b directions but no difference could be distinguished within the experimental accuracy. This is in agreement with the theoretical interpretation which predicts a basal plane anisotropy of less than 0.8% at the highest field.

Isothermal magnetization measurements in the a and b directions in Y-Er (Fig. 6) revealed an anisotropy of about 2.2% at low temperatures and high field with the a direction as the easy direction.

The empty sampleholder uncertainty is important in the isotherms in the c direction at low temperatures in Y-Dy (Fig. 7) since this direction is magnetically very hard. The deviations of the low-temperature isotherms from the theoretical curves will be discussed later.

The high-field isofield curves (Figs. 8–10) show the same general features as the low-field susceptibility curves. However, the nonlinearity parameter t, defined as $t=\chi_0/\chi_{HF}-1$, where $\chi_0=dM/dH$, $H=0$, and $\chi_{HF}=M/H$, $H=44.2\times10^5$ A/m, deviates considerably from zero in some cases (Figs. 8 and 10).

HEXAGONAL-CRYSTALLINE-FIELD FITS

In a hexagonal-close-packed lattice the most general operator describing any single-ion interaction within a manifold of given J for a $4f$ ion reads

$$\mathcal{H}_{CF}=B_{20}\,O_{20}+B_{40}\,O_{40}+B_{60}\,O_{60}+B_{66}\,O_{66}\ . \qquad (1)$$

O_{lm} are Stevens operators as given by Abragam and Bleaney.[7(a)] B_{lm} are the crystalline-field parameters.

In (1) it is assumed that the c axis and the z direction coincide, and we take the x and y directions

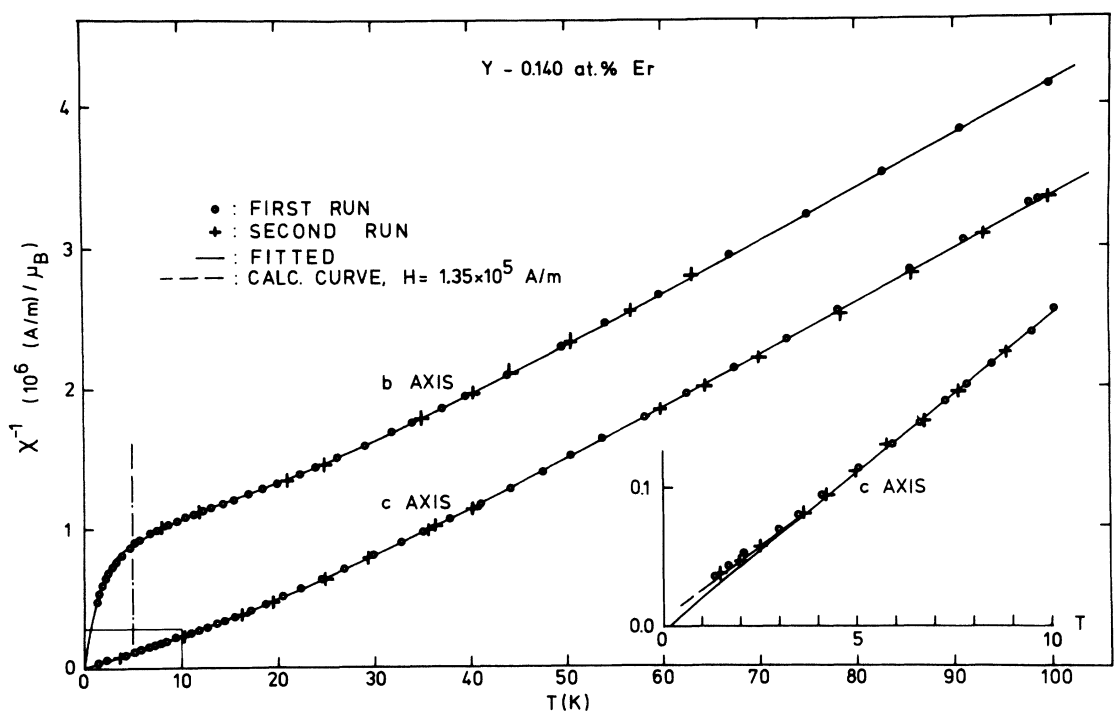

FIG. 2. Reciprocal susceptibility of Y–0.140-at.% Er. (Faraday measurements at 1.35×10^5 A/m.) The theoretical curves are fitted to the first-run data with a cutoff temperature $T_{min}=5$ K. The parameters are shown in Table III.

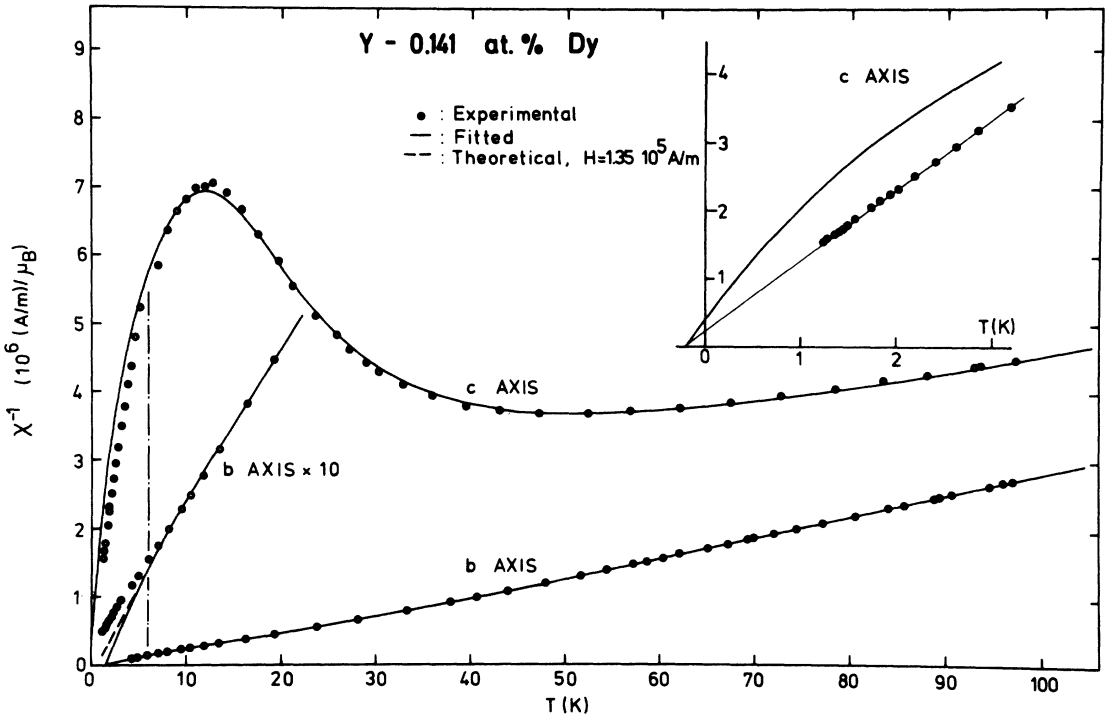

FIG. 3. Reciprocal susceptibility for Y–0.141-at.% Dy. (Faraday at 1.35×10^5 A/m.) The fitted curves are obtained with a cutoff temperature $T_{min}=6$ K. The parameters are given in Table III.

as along a and b axes, respectively.

When k_BT is very much smaller than the distance from the ground multiplet to the first-excited manifold, as is the case for Er (9500 K) and Dy (5100 K), the zero-field susceptibility of a $4f$ ion is

$$\chi_H^{CF}=(g_J\mu_B)^2\frac{\sum_n\sum_m{}'|\langle n|J_H|m\rangle|^2e^{-E_n/k_BT}}{\sum_n e^{-E_n/k_BT}}\frac{1}{k_BT}-2(g_J\mu_B)^2\frac{\sum_n\sum_m{}''|\langle n|J_H|m\rangle|^2(E_n-E_m)^{-1}e^{-E_n/k_BT}}{\sum_n e^{-E_n/k_BT}}. \quad (2)$$

Here g_J is the appropriate Landé factor, μ_B is the Bohr magneton, k_B is the Boltzmann constant, and J_H is the component of the angular momentum operator in the direction of the field. $|n\rangle$ and E_n are the eigenfunctions and energies of the crystalline-field operator $\mathcal{H}_{CF}$. The summation $\sum_m'$ is carried out only over states $|m\rangle$ with $E_m=E_n$, whereas $\sum_m''$ includes all other states. A computer program was written which diagonalizes $\mathcal{H}_{CF}$ and computes χ^{CF} according to (2).

For very dilute alloys, exchange-interaction ef-

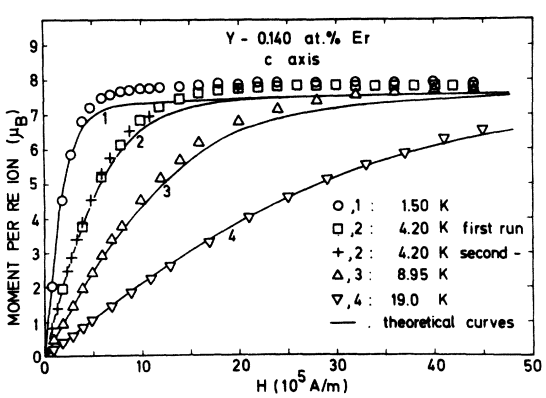

FIG. 4. Isotherms for Y–0.140-at.% Er in the c direction (Faraday).

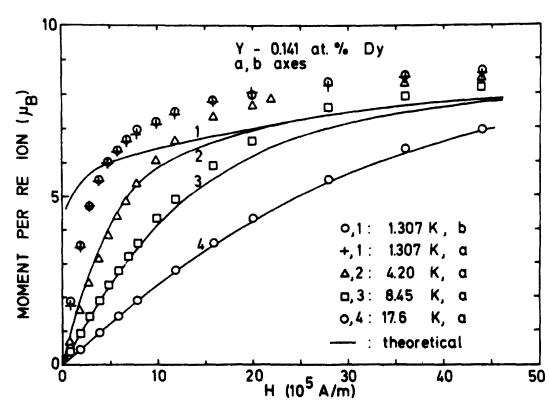

FIG. 5. Isotherms for Y–0.141-at.% Dy, basal plane (Faraday).

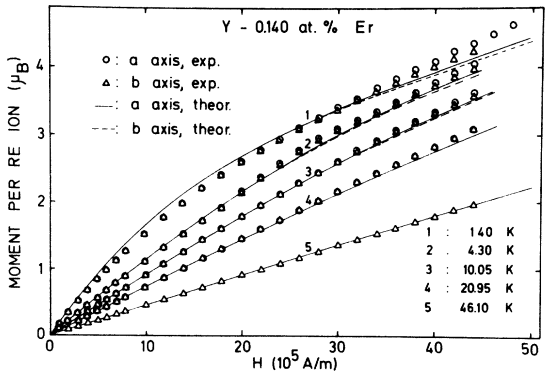

FIG. 6. Isotherms for Y–0.140-at.% Er in the basal plane (VSM).

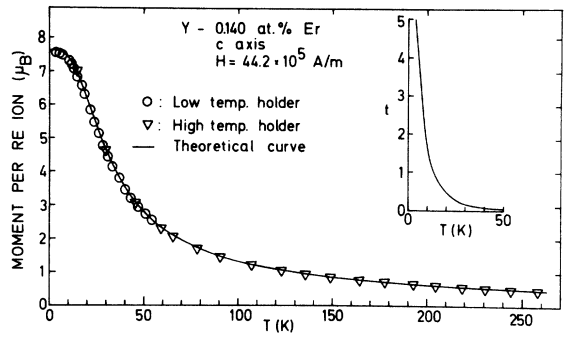

FIG. 8. Isofield curve at 44.2×10^5 A/m in the c direction for Y–0.140-at.% Er (VSM). The nonlinearity parameter $t=(\chi_0/\chi_{HF})-1$, $\chi_0=dM/dH$ at $H=0$ and $\chi_{HF}=M/H$ at $H=44.2\times10^5$ A/m.

fects are expected to be small; they were therefore taken into account in the molecular-field approximation:

$$\frac{1}{\chi_{expt}}=\frac{1}{\chi_{CF}}-\gamma\ . \tag{3}$$

A positive γ means ferromagnetic coupling.

The computer program performs a least-squares fit to the reciprocal susceptibilities in the c direction (z) and in the basal plane (x), simultaneously. The parameters used in the fit are B_{20}, B_{40}, B_{60}, B_{66}, γ_z, γ_x, and c, where c is the concentration.

The normalized least-squares deviation

$$S=\frac{\langle(1/\chi_{theor}-1/\chi_{expt})^2\rangle}{\langle(1/\chi_{theor})^2\rangle}$$

was used as fitting criterion. The terms in S were weighted appropriate to an error in $1/\chi$ proportional to $1/\chi$ and, in order to get a rapid convergence the method of steepest descents was used for the parameters B_{lm}.

In anticipation of short-range-order effects we performed a series of fits in which the lowest-temperature data were disregarded. As the cutoff temperature was lowered, a small decrease in S was observed until a minimum was reached at a certain temperature T_{min}, below which S started to rise rapidly. The best fit was taken to be that giving the smallest value of S.

For Er we obtained $S_{min}^{1/2}=0.46\%$ and for Dy $S_{min}^{1/2}=1.0\%$; these values indicate that the fits in both cases are as good as the experimental accuracy allows.

The parameters B_{lm} varied little as the cutoff temperature was lowered. The stated errors of the parameters are estimated from this variation. These errors are one order of magnitude larger than those obtained from the sharpness of the minimum in the least-squares deviation.

As we have used a zero-field expression for χ,

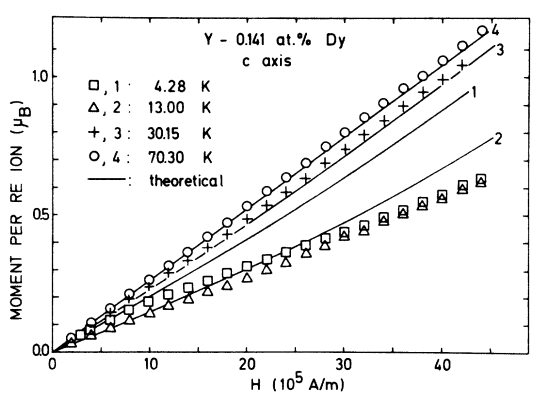

FIG. 7. Isotherms in the c direction for Y–0.141-at.% Dy (VSM). The inaccuracy owing to the nonreproducibility of the sample-holder contribution is $\pm1.5\times10^{-2}$ μ_B.

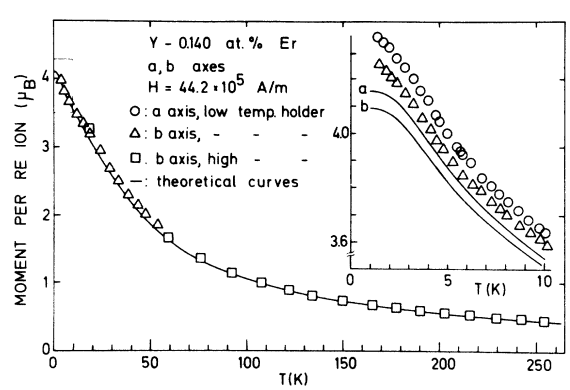

FIG. 9. Isofield curves at 44.2×10^5 A/m in the basal plane for Y–0.140-at.% Er.

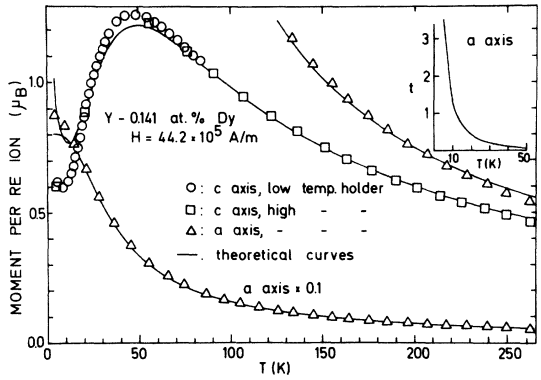

FIG. 10. Isofield curves at 44.2×10^5 A/m for Y–0.141-at.% Dy (VSM). The nonlinearity parameter t is also shown.

we always checked that the correction for finite field of the susceptibility measurements was negligible for $T \geq T_{min}$.

Erbium

Owing to the marked deviations from a Curie–Weiss type of susceptibility (Fig. 2) we had no difficulty in determining the crystalline-field parameters, contrary to the (cubic) case of Ag-Er and Au-Er.[8] To avoid any ambiguity we calculated the susceptibility in a parameter range of several orders of magnitude for all parameters and for all signs of B_{40} and B_{60}. The calculation indicated three local minima in S. Each minimum was examined and it turned out that the one with the smallest value of S_{min} was the only one which led to reasonable agreement with the measured high-field isofield curves.

The values found for B_{lm} are given in Table III. The higher-order terms in (1), B_{40}, B_{60}, and B_{66}, were found to be more important than expected in the simple point-charge model. The over-all splitting is 130 K, the B_{20} term alone accounting for 52 K. Furthermore, $B_{20}O_{20}$ alone would cause the

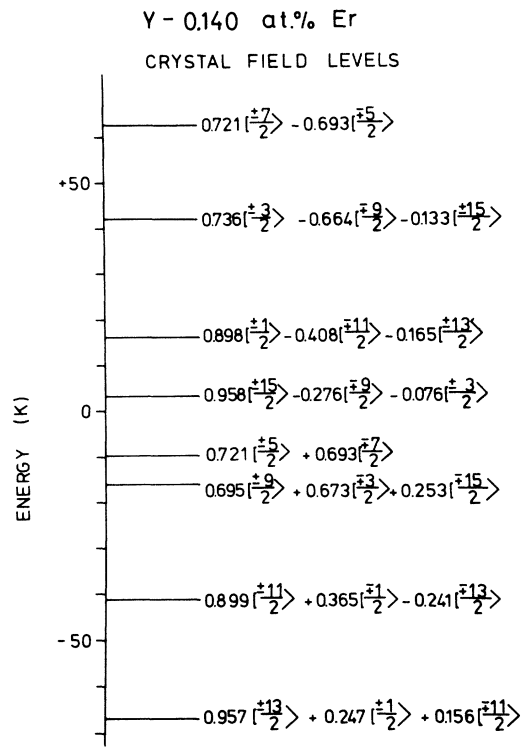

FIG. 11. Energies and eigenfunctions for Y–0.140-at.% Er.

ground-state doublet to be $|\pm\frac{15}{2}\rangle$. However, this state (with a little admixture of $|\pm\frac{3}{2}\rangle$ and $|\mp\frac{9}{2}\rangle$) is found to lie in the middle of the multiplet. The ground state is $0.957\,|\pm\frac{13}{2}\rangle + 0.247\,|\pm\frac{1}{2}\rangle + 0.156\,|\mp\frac{11}{2}\rangle$, as shown in Fig. 11. The g factors for this doublet are $g_{\parallel} = 14.02$ and $g_{\perp} = 2.48$. ESR measurements are under preparation to confirm this assignment and the results will be published elsewhere.

The next excited state is a doublet of the same type as the ground state, but it is dominated by $|\pm\frac{11}{2}\rangle$. The separation between the two lowest pairs of states is 26 K.

TABLE III. Values of fitted parameters.

Parameter	Units	Dy	Er
B_{20}	K	$+0.321 \pm 10\%$	$-0.309 \pm 10\%$
B_{40}	K	$-0.293\times10^{-2} \pm 10\%$	$+0.814\times10^{-3} \pm 10\%$
B_{60}	K	$+0.418\times10^{-4} \pm 10\%$	$+0.243\times10^{-4} \pm 10\%$
B_{66}	K	$-0.333\times10^{-3} \pm 10\%$	$-0.279\times10^{-3} \pm 10\%$
θ_z	K	-0.20 ± 0.06	$+0.15 \pm 0.07$
θ_x	K	$+1.6 \pm 0.2$	$+0.13 \pm 0.07$
γ_z	10^5(A/m)/μ_B	$-3.7 \pm 30\%$	$+0.042 \pm 50\%$
γ_x	10^5(A/m)/μ_B	$+0.64 \pm 15\%$	$+0.62 \pm 50\%$
c	at.%	0.141 ± 0.001	0.140 ± 0.001
Nom. conc.	at.%	0.134	0.142

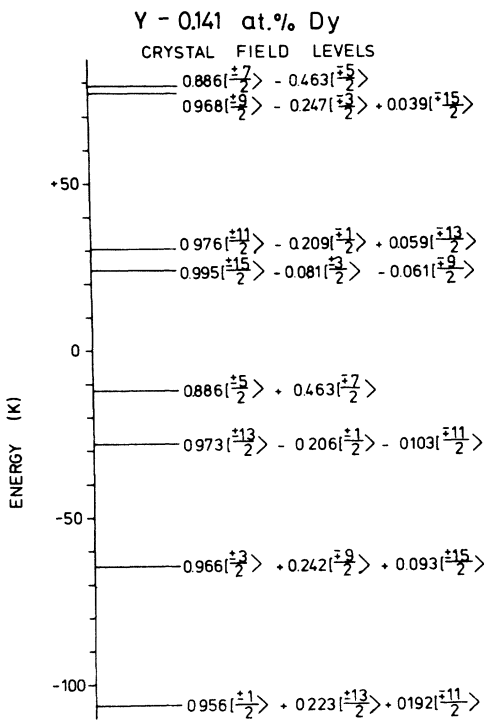

FIG. 12. Energies and eigenfunctions for Y–0.141-at.% Dy.

Exchange interactions were found to be of little importance in Y-Er. Expected ordering temperatures are of the order of 0.1 K (Fig. 2). The γ's are ferromagnetic in both the c and b directions with a large anisotropy but the paramagnetic Curie temperatures are isotropic, θ_b being 0.13 ± 0.07 K and $\theta_c = 0.15 \pm 0.07$ K.

The deviation below 5 K between the experimental points and the theoretical susceptibility curve in the c direction (Fig. 2) can be accounted for completely by the nonlinearity of the isotherms.

Isofield curves for $H = 44.2 \times 10^5$ A/m were calculated in the a, b, and c direction by diagonalizing a Hamiltonian containing the Zeeman interaction and the crystalline-field operator (1). The exchange interaction was treated in the molecular-field approximation.

The anisotropy in the basal plane (Fig. 9) is found to agree well with experiment, thus providing a check on the value of $|B_{66}|$. The sign of B_{66} is negative.

In the c direction the nonlinearity parameter t defined above varies from 5.50 at 2 K to 0.17 at 30 K (Fig. 8). The isofield curve in this direction thus provides a good check on the crystalline parameters. As seen from the figure the measured and calculated values agree within 3%.

Isotherms were calculated in the same way as the isofield curves. The calculated moment in the c direction at 44.2×10^5 A/m is $7.60 \mu_B$/(RE atom) compared to the experimental value $7.94 \mu_B$/(RE atom), both at 1.5 K (Fig. 4). The difference is presumably due to ferromagnetic enhancement caused by polarization of the conduction electrons. The enhancement factor is 1.045.

The isotherms in the a and b directions (Fig. 6) show an enhancement of the same order of magnitude.

Dysprosium

The deviations from a Curie–Weiss type of susceptibility are even more pronounced in Y-Dy (Fig. 3). The ground state is an almost pure $|\pm\frac{1}{2}\rangle$ doublet with an axial g tensor: $g_{\parallel} = 1.54$ and $g_{\perp} = 10.05$, thus making ESR measurements possible. The next excited doublet is an almost pure $|\pm\frac{3}{2}\rangle$ state 42 K

TABLE IV. Comparison between theoretical and different experimental values. The values from Refs. 10–13 are from measurements on pure Dy and Er. Those from Ref. 14 are deduced from measurements on Gd doped with the rare earths. The column "corr for c/a" gives the values from this paper corrected for the different c/a ratios of Y, Dy, and Er according to the formulas of Kasuya (Ref. 15). Values are in K/(RE atom).

Dy Ref.	10	11	14	12	This paper	corr. for c/a	15 (theory)
$A_{20}\langle r^2\rangle$	−172	−320	−105	−115	−50	−51	−115
$A_{40}\langle r^4\rangle$			−6		+50	+49	−7
$A_{60}\langle r^6\rangle$			+3		+40	+40	+4
$A_{66}\langle r^6\rangle$	29				−321	−321	−32

Er Ref.	13	14	This paper	corr. for c/a	15 (theory)
$A_{20}\langle r^2\rangle$	−162	−96	−122	−131	−114
$A_{40}\langle r^4\rangle$		+6	+18	+17	−6
$A_{60}\langle r^6\rangle$		+2	+12	+12	+3
$A_{66}\langle r^6\rangle$			−135	−135	−26

TABLE V. Values of $A_{lm}\langle r_{4f}^{l}\rangle$ in units of K and ratios.

lm	Dy	Er	Ratio
20	−50	−122	+0.41
40	+50	+18.3	+2.7
60	+40	+11.7	+3.4
66	−321	−135	+2.4

above the ground state (Fig. 12).

In Y-Dy exchange interactions are found to be much more important than in Y-Er. In the easy direction we find a paramagnetic Curie temperature of $\theta_b = +1.6 \pm 0.1$ K, whereas in the c direction we find $\theta_c = -0.20 \pm 0.03$ K (Fig. 3).

The difference at low temperatures between the experimental and theoretical reciprocal susceptibility (Fig. 3) is equally due to exchange effects and the nonlinearity of the isotherms. The high-field isofield curves shown in Fig. 10 exhibit reasonable agreement with experiment.

Owing to the rather high ordering temperature in Dy the molecular-field approximation is not adequate at temperatures in the range of 1 K as can be seen from the isotherms in Fig. 5. At 4.2 K we find an enhancement of 10.5% at $H = 44.2\times10^5$ A/m. The calculated anisotropy in the basal plane is less than 0.8%.

The isotherms in the c direction (Fig. 9) give smaller moments than calculated. Especially the 4.28-K curve deviates more than could be accounted for by the uncertainty in the experimental points. This deviation cannot be accounted for by any crystal-field effects.

DISCUSSION

The excellent consistency between experimental and theoretical values, except at low temperatures where ordering effects become important, indicates the validity of the general single-ion Hamiltonian (1), and shows that the alloy concentrations chosen were appropriate for this experiment. In Table III all the fitted parameters and their accuracies are summarized. To get more information about the exchange constants it would be valuable to make susceptibility measurements at different concentrations. Such experiments are being planned.

The crystalline potential which acts on an electron may be written in the r representation [7(b)]:

$$V(\bar{x}) = \sum_{l,m} A_{lm} P_{lm}(\bar{x}) .$$

P_{lm} are unnormalized homogeneous polynomials of degree l, and A_{lm} are parameters which characterize the potential.

The effect of the potential on a RE ion can be accounted for by the operator of Eq. (1), where the parameters B_{lm} are proportional to the potential parameters A_{lm},

$$B_{lm} = A_{lm}\langle r_{4f}^{l}\rangle \langle J||\alpha_l||J\rangle .$$

Here $\langle r_{4f}^{l}\rangle$ is the mean value of the $4f$-electron radius raised to the lth power and $\langle J||\alpha_l||J\rangle$ is the Stevens factor,[7(c)] which depends on the actual quantum numbers of the RE ion.

In Table IV we first compare the $A_{lm}\langle r_{4f}^{l}\rangle$ which we obtain with those deduced from other experimental data. Disagreements are attributed to anisotropic exchange, the importance of which Nicklow *et al.*[9] have pointed out for the case of Er, and magnetoelastic contributions to the anisotropy. The values calculated in a simple point-charge model also shown in Table IV differ by up to a factor 10 from the values found in this paper and even differ in sign for A_{40} for both Dy and Er. In Table V the ratios of $A_{lm}\langle r_{4f}^{l}\rangle$ for Dy to those of Er are shown.

If the A_{lm}'s were specific for the Y host these ratios should, owing to the similarities of Dy and Er with respect to $4f$ radii, be approximately unity. As this is clearly not the case it seems that charges on the impurity itself play a crucial role in determining the potential acting on the $4f$-impurity electrons. Williams and Hirst,[8] who have come to a similar conclusion for rare-earth doped in Ag or Au, have suggested a model for the crystal field based on the hypothesis of a nonmagnetic $5d$ virtual bound state on the rare earth.

In order to check the validity of the crystal-field parameters found from the magnetization measurements we have initiated further experiments including: (a) determination of B_{66} separately by a basal-plane anisotropy measurement, (b) magnetization measurements up to high fields (40 T), (c) neutron spectroscopy, and (d) ESR spectroscopy.

We are also studying dilute alloys of Lu-Re to compare crystal fields for these alloys with those found in Y-RE. The results of these measurements will be presented in due course.

ACKNOWLEDGMENTS

The authors gratefully acknowledge the invaluable help of Torben Johansson in the experimental part of the project. They also wish to thank Professor V. Frank and Professor A. R. Mackintosh for their continued interest and their careful reading of the manuscript.

[1]K. N. R. Taylor and M. I. Darby, *Physics of Rare Earth Solids* (Chapman and Hall, London, 1972).
[2]T. Sugaware and R. J. Soga, J. Phys. Soc. Jap. 18, 1102 (1963).
[3]K. A. McEwen and P. Touborg, J. Phys. F 3, 1903 (1973).

[4]H. E. Nigh, J. Appl. Phys. 45, 3323 (1963).
[5]J. Crangle and G. M. Goodman, Proc. R. Soc. Lond. A 321, 477 (1971).
[6]D. K. Wohlleben, Ph.D. thesis (University of California, San Diego, 1968) (unpublished).
[7](a) A. Abragam and B. Bleaney, *Electron Paramagnetic Resonance of Transition Ions* (Oxford U. P., Oxford, England, 1970), pp. 864–872; (b) p. 669, Eq. (16.10) and Table 15; (c) p. 874, Table 20: Here $\langle J||\alpha_2||J\rangle = \langle J||\alpha||J\rangle$, $\langle J||\alpha_4||J\rangle = \langle J||\beta||J\rangle$, and $\langle J||\alpha_6||J\rangle = \langle J||\gamma||J\rangle$.
[8]G. Williams and L. L. Hirst, Phys. Rev. 185, 407 (1969).
[9]R. M. Nicklow, N. Wakabayashi, M. K. Wilkinson, and R. E. Reed, Phys. Rev. Lett. 27, 334 (1971).
[10]J. J. Rhyne and A. E. Clark, J. Appl. Phys. 38, 1379 (1967).
[11]P. H. Bly, W. D. Corner, and K. N. R. Taylor, J. Appl. Phys. 40, 4787 (1969).
[12]P. Touborg and S. Balling, unpublished paramagnetic measurements.
[13]P. Touborg and K. M. Ravn, unpublished paramagnetic measurements.
[14]S. Chikazumi, K. Tajima, and K. Toyama, J. Phys. (Paris) 32, C1-180 (1971).
[15]T. Kasuya, in *Magnetism*, edited by G. T. Rado and H. Suhl (Academic, New York, 1966), Vol. 2B.